

Assessment of Interaction Diagrams for Cyclic Axial Loads in Offshore Piles Based on an Effective Stress Method. A Gulf of Mexico Case

J. G. PARRA^{a,1} and M. GUEVARA^b

^a*Geosciences VP, GEOHIDRA, Caracas, Venezuela*

^b*Geosciences Project Engineer, GEOHIDRA, Caracas, Venezuela*

Abstract. Cyclic axial loads effects have long been recognized as one of the most significant actions that pile foundations of offshore structures have to withstand during its useful life. In spite of that there is no consensus in the best approach to assess its effects. In this work the CPT-based effective stress ICP (Imperial College Pile) method was used to evaluate the cyclic axial resistance by suitably combining it with an accumulation procedure that progressively accounts for the local reduction in radial effective stress acting on the shaft. In the first stage the soils involved were characterized in terms of the reduction of effective stress observed in Cyclic Direct Simple Shear tests (DSS, ASTM D6528). Secondly, following the ICP method, the reduction in axial load is computed from the local reduction of the effective radial stress along the pile shaft. This involves the discretization of piles with elastoplastic degrading t-z curves. The global effect along the pile is computed and the results are summarized in terms of cyclic interaction diagrams. The procedure provides a robust approach that considers the main aspects of cyclic response, including the progressive degradation of resistance along the shaft during the load history. This procedure was applied to a real case of piles driven in a variable soil profile in the Mexican Gulf of Mexico area.

Keywords. Cyclic axial loads, ICP method, cyclic resistance interaction diagrams.

1. Introduction

Cyclic axial loads have long been recognized as one of the most significant actions that pile foundations of offshore structures have to withstand during its useful life. In spite of that there is no consensus in the best approach to assess its effects. For clays, methods based in total stresses and empirical degradation factors applied to the undrained shear strengths are typically used [1]. More recently methods based on evaluating the reduction in effective stress along the pile shaft have been proposed [2, 3]. The main advantage of the effective stress methods is that they can be applied to both sands, clays and intermediate materials with the proper precautions. In this work the CPT-based effective stress ICP (Imperial College Pile) method was used to evaluate the cyclic axial resistance by suitably combining it with an accumulation procedure that progressively accounts for the local reduction in radial effective stress acting on the shaft. For a given pile geometry

¹ Corresponding Author: Jose G Parra. Edif Geohidra. Calle Razetti. Urb Los Chaguaramos. Caracas 1040. Venezuela. E-mail:jparra@geohidra.com

and soil profile the results are summarized in cyclic interaction diagrams that allow a rapid quantification of cyclic degradation.

2. The ICP method

The ICP (Imperial College Pile) method is an effective stress pile design method. The method is thoroughly described in [3]. Essentially the method proposes a Coulomb failure criterion for the local (at any depth z of interest) vertical shear stress at failure acting along the pile shaft:

$$\tau_{rzf} = \sigma'_{rrf} * \tan(\delta_f) \tag{1}$$

where τ_{rzf} is the (vertical) shear stress at failure acting on the shaft, σ'_{rrf} the normal to the shaft (radial) effective stress at failure and δ_f the operational interface angle of friction at failure². σ'_{rrf} is obtained from σ'_{rrc} , the radial effective stress acting after equalization, i.e. after any change in pore pressure during installation has dissipated but before any long term effect (creep, ageing) has had time to act. For sands a dilatant increase during pile loading is assumed to occur ($\sigma'_{rrf} = \sigma'_{rrc} + \Delta\sigma'_{rr}$); for clays a decrease is assumed ($\sigma'_{rrf} = 0.8 * \sigma'_{rrc}$). σ'_{rrc} is obtained from σ'_{zZo} , the in situ free field vertical effective stress, and CPTU values (for sands), or from Yield Strength Ratio and Sensitivity for clays. The method provides a unified conceptual framework for dealing with both clays and sands. It has been shown to provide good results for a wide variety of soils conditions and intermediate soils [3, 4]. The ICP method is one of the CPT-based methods recommended for sands in the latest edition of the API RP2GEO [5] and ISO 19901-4.

3. Cyclic Axial load capacity interaction diagrams

A cyclic interaction diagram shows the combinations of “average” axial load (Qa) and cyclic load (Qc) that would cause pile failure under a given number of cycles (N) of constant amplitude ±Qc (Figure 1a,1b). Typically the results are normalized either by the total static shaft resistance or the total static capacity (shaft + tip resistance), the latter option used in this article. Implicit in their use is a proper definition of “failure”, which in the present work is assumed to occur when the maximum applied total cyclic load (Qa+Qc) is just equal to the current (and reduced) post cyclic capacity. Alternative definitions of failure in terms of maximum ultimate displacements are also possible. Figures 1a and 1b show two examples of cyclic interaction diagrams interpreted from field tests in sands [2]. If no degradation was produced the diagrams would collapse in the main diagonal (from upper left corner to lower right corner).

No inertial effects are included in this work. If radiation damping is considered relevant its effect can be approximately considered by the use of discrete dashpots. Strain rate effects can also be independently incorporated, see for instance [1, 6].

² z,r refers to a cylindrical coordinate system: z depth along pile axis, r: radial direction from pile axis.

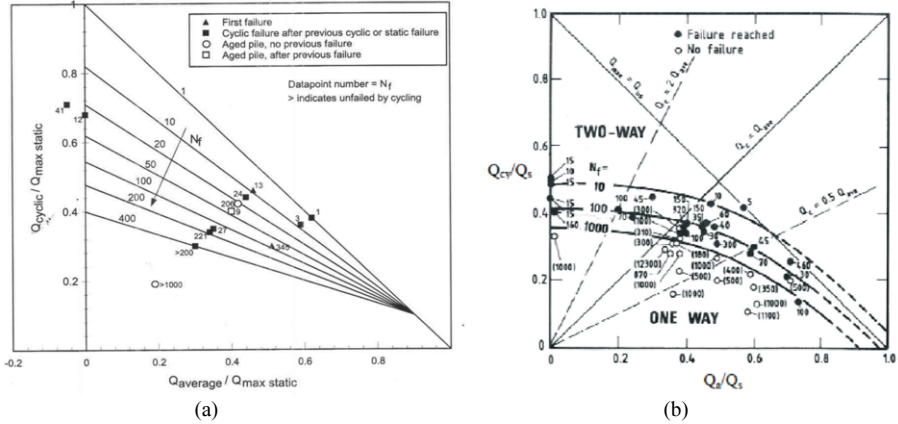


Figure 1. Examples of cyclic interaction diagrams: (a) Dunkirk sand; (b) Haga clay, Ref [2].

4. Computation of pile response to the application of cyclic axial loads

Although the main variables affecting the response of piles to cyclic axial loads are reasonably well understood there is no consensus in the most effective way to properly assess it [1, 2, 6]. In the present work the computation of the pile response to static and/or cyclic axial loads is based on the “classic” discretization of the pile in linear beam-column elements. The interacting surrounding soil is modelled with elastoplastic and *degrading* t-z (shaft) and Q-z (pile tip, non-degrading) spring-like elements. For the static case a simplified bi-linear shape of the t-z and Q-z elements derived from those given in API RP2GEO [5] are used, without the post peak reduction of “t” values for clays. The maximum shaft resistances along the pile (“t”) and the pile tip resistance (“Q”) are obtained from the ICP method.

The cyclic t-z curves are assumed to have a standard elastic perfectly plastic hysteretic response but with progressively decreasing maximum yield (t_{max}) values. Although these softening or degradation occurs progressively as the cyclic action develops, following Ref [7] is assumed that the degradation occurs discretely, after a given number of cycles have acted on the t-z element.

4.1. Pile response with elastoplastic non-degrading t-z curves

The computation of the pile response to a prescribed total axial load history applied at the pile head follows the standard structural algorithms where the complete stiffness matrix of the pile-soil system is derived from the individual pile segments matrices (assumed linear) and for each of the t-z elements elastoplastic stiffness relation. In order to capture the loading-unloading behavior the standard one-dimensional incremental plasticity algorithm with an elastic predictor step and return mapping, as described in for instance Refs. [8, 9] is applied explicitly to the t-z and Q-z elements. If a constant amplitude cyclic axial load were applied, after a relatively small number of cycles the amplitudes of the shaft shear stresses (“t”) at each element would reach a steady state (shakedown) value.

4.2. Model of local shaft resistance degradation

The accumulation of the cyclic action produces a reduction in the radial effective stress (normal to the pile wall) and hence in the maximum shaft resistance, which leads to a progressively softer response of the complete pile-soil system. The reduction in maximum shaft resistance at a given location (and given t-z element) is computed from the reduction in normal effective stress, as obtained from constant volume (i.e. constant height), cyclic direct simple shear tests (CDSS, ASTM D6528) on nominally intact samples of clays and/or reconstituted sand samples subjected to a controlled constant amplitude of cyclic shear stress. For sands the condition of constant volume may be too conservative, alternatively a Constant Normal Stiffness could be used, which models the high radial stiffness of the sand beyond the shaft [2,3]. Following Ref [3, 7] the reduction in normal effective stress for each element, which affects the σ'_{rrf} term in Eq. (1), can be expressed as:

$$r = -\frac{\Delta\sigma'_n}{\sigma'_{no}} = f\left(\frac{\tau_{cyc}}{\tau_{max\ static}}, N\right) \quad \text{laboratory} \quad (2)$$

$$r = -\frac{\Delta\sigma'_{rr}}{\sigma'_{rc}} = f\left(\frac{\tau_{rz,cyc}}{\tau_{rz\ max\ static}}, N\right) \quad \text{pile} \quad (3)$$

In Eq. (2) $\Delta\sigma'_n$ is the reduction in the normal effective stress, σ'_{no} the effective stress at which the sample was consolidated (in the lab), τ_{cyc} the amplitude of constant two-way symmetric shear stress applied in the laboratory, $\tau_{max\ static}$ the maximum static shear strength at the pile-soil interface and N the total number of cycles. Eq. (3) is the same but with the corresponding stresses directions in the pile element. These equations assume that the average acting shear stress (τ_{avg}) has negligible effect on the degradation response, which needs to be verified in each case.

4.3. Accumulation of shaft resistance degradation

As explained in Ref [7], Eqs. (2) and (3) cannot be applied directly at the element level in the pile-soil system because the cyclic amplitude (τ_{cyc}) in each t-z element is not constant along the load history (in this work what is constant is the cyclic component of the total axial load at the pile head). As the load history progresses the maximum value of shaft resistance in each t-z element decreases, which causes redistribution of the shaft stresses from the upper zones of the pile (assumed weaker) towards the deeper zones. In order to account for this effect Ref [7] divides the N cycles of total axial load in *m* blocks of N/m cycles each (m in the order of 3 to 10). During the first block of N/m cycles the t-z curves are assumed to be equal to the static ones and to remain undegraded. From this and following the one-dimensional elastoplastic algorithm the amplitudes τ_{cyc1} of the cyclic stress in each t-z element representative of the response in the first block are computed. These amplitudes are used to compute the reduction in the effective radial stress (Eq. (3) with N/m cycles) and hence the new degraded maximum t values for the start of the second block. For the second block of N/m cycles the new amplitudes τ_{cyc2} of the cyclic stress in each t-z element are again computed. From this point on is necessary to accumulate the degradation due to the first N/m cycles of amplitude τ_{cyc1} and the second N/m cycles of (different and possibly larger) amplitude τ_{cyc2} . Ref [7] uses an accumulation procedure proposed by Ref [10]. In this work an alternative approach based

on the proposal by [11] is used. The first N/m cycles at amplitude τ_{cyc1} are “transformed” in N_1 equivalent cycles at amplitude τ_{cyc2} that produce the same degradation (reduction in effective stress) using Eq. (3):

$$f\left(\frac{\tau_{cyc1}}{\tau_{rz \max static}}, N/m\right) = f\left(\frac{\tau_{cyc2}}{\tau_{rz \max static}}, N_1\right) \quad (4)$$

The total degradation after the second block is then calculated for N_1+N/m cycles at amplitude τ_{cyc2} (N_1+N/m varies for each t - z curve). These degraded t - z curves are used for the start of the third block. The process is repeated for the remaining blocks up to m . As explained in 4.1 it is not necessary to compute the response during the total load history in each block “ i ” ($i=1\dots m$), only until the steady state is reached. The algorithm is relatively insensitive to the number m of blocks, providing m is not too small (see 5.2).

4.4. Pile response with degrading t - z curves

For a given amplitude of Q_a and Q_c the above described procedure would produce a set of degraded t - z elements after each block “ i ” of N/m cycles ($i=1, 2, \dots, m-1, m$). As the problem is formulated assuming load control, the computation would fail to converge if at any block Q_a+Q_c is greater than the current degraded total axial capacity at the start of the block. For a given Q_a , Q_c is progressively increased until the post cyclic capacity at the end of the last block ($i=m$) is just equal to Q_a+Q_c . Then both values of Q_a and Q_c are plotted in the cyclic interaction diagram.

5. Application to a case in the Campeche area of Gulf of México

Following is an example of the proposed methodology to a case in the Bay of Campeche area in the Mexican sector of Gulf of Mexico. The soil profile in this example consists of a surficial very soft to soft high plasticity normally consolidated clay of 12 m thickness, followed by an alternating sequence of medium and low plasticity, moderately overconsolidated clays alternated with sands and silty sands. The consistency of the clays increases with depth, from stiff at about 12 m depth to hard at 120 m. The sands strata alternate with the clays strata in varying thickness from 3 to 9 m. Their relative density increases with depth from medium at about 15 m to dense at about 100 m. The sand strata comprises about 40% of the profile from 12 to 120 m.

5.1. Shaft resistance degradation

As explained in 4.2 the shaft resistance degradation was obtained from the reduction in normal effective stress, as obtained from constant volume CDSS tests, at a frequency of 1 Hz, on nominally intact samples of clays and/or reconstituted sand samples subjected to a controlled constant amplitude of cyclic shear stress [12] For the sands, after an initial consolidation to the selected effective stress a preshearing of 200 to 400 cycles with an amplitude of about 10% of the maximum shear strength was applied, followed by a new consolidation at the same effective stress. Due to this the sands compacted 0.1 to 0.2% of the initial total volume. Additional sets of DSS tests at increasing strain rate showed a negligible increase of shear strength for the soils in this case, even for the clays. A typical shear stress vs effective normal stress diagram is shown in Figure 2. The results of the set of tests can be summarized in the following equations ($0 < r < 1$) (Figure 3 and 4):

- For clays:

$$r = -\frac{\Delta\sigma'_{rr}}{\sigma'_{rrc}} = 0.06161 \left(-0.02133 + 1.3818 * \frac{\tau_{rz,cyc}}{\tau_{rz \max static}} \right) N^{0.2157} < 1 \quad (5)$$

- For sands:

$$r = -\frac{\Delta\sigma'_{rr}}{\sigma'_{rrc}} = 0.3761 \left(-0.1196 + 3.5117 * \frac{\tau_{rz,cyc}}{\tau_{rz \max static}} \right) N^{0.1593} < 1 \quad (6)$$

- Alternatively for sands

$$r = -\frac{\Delta\sigma'_{rr}}{\sigma'_{rrc}} = 1.516 \left(\frac{\tau_{rz,cyc}}{\tau_{rz \max static}} \right)^{2.00} N^{0.400} < 1 \quad (7)$$

As expected, the degradation in the clays is significantly lower than in the sands. For the sands, two expressions are presented: they differ in the degree of approximation to the experimental values, and represent a different compromise either in the regions of low or high numbers (N) of cycles. The experimental results show a substantial degree of cyclic degradation of the sands with a relatively small number of cycles (N~15-30) for shear stress amplitudes of 30% or more of the maximum static strength. Similar results are reported by the Instituto Mexicano del Petróleo [13] for shallow sands (depths less than 30 m) in strain controlled cyclic tests used as part of the study of the free field response of soil deposits in the same area to seismic action.

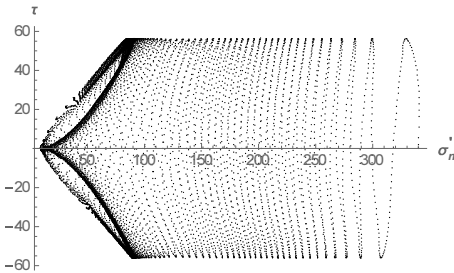


Figure 2. Examples of stress controlled cyclic DSS test.

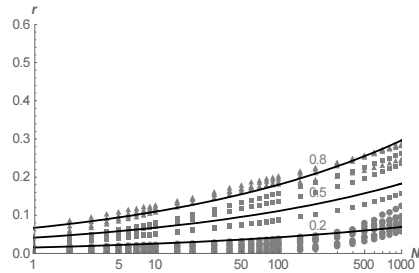
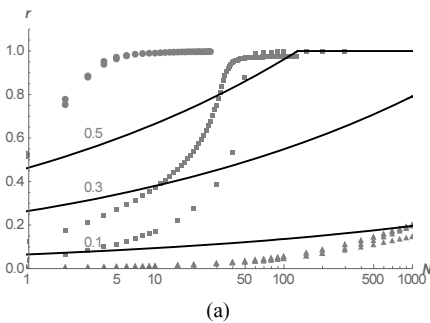
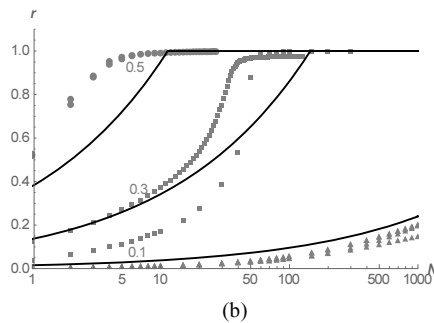


Figure 3. Clay degradation model.



(a)



(b)

Figure 4. Sand degradation models: (a) Eq. (6); (b) Eq. (7).

5.2. Results for 15, 100, 1000 cycles

For a given soil profile in principle the cyclic interaction diagram is unique for each pile diameter, wall thickness and length. The diagrams were calculated for piles of 1.5” wall thickness, diameters of 36”, 48” and 66” and a length equal to approximately the maximum length explored minus 3 diameters (115 m).

Firstly, for a given N the sensitivity of the results to the number of blocks (m) is investigated. Figure 5 shows the degradation of total post cyclic axial resistance after each block for three cases: m=4 (N=4*250), m=10 (N=10*100) and m=25 (N=25*40) blocks for a total of N=1000 cycles in each case. It can be seen that the results are approximately insensitive to a reasonable choice of the number of blocks (m) in which the total number of cycles (N) is divided.

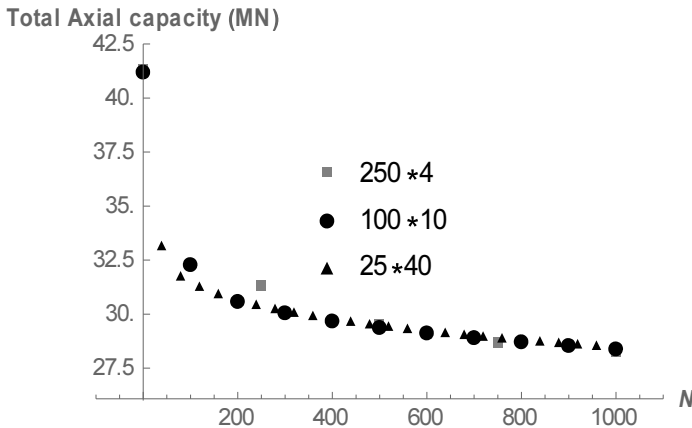


Figure 5. Sensitivity of results to the number “m” of blocks.

For the sand degradation given by Eq. (6) the diagrams were calculated for N=15, 100 and 1000 cycles, and are presented in Figure 6. The following observations are noted: i) the results are insensitive to the pile diameter (both Q_c and Q_a are normalized by their respective Q_s); ii) a high proportion of the total degradation occurs in the first 15 cycles of axial load, the reduction is of the order of 45-40% and slightly decreasing with the average axial load (Q_a); iii) increasing the number of cycles from N=15 to N=1000 reduces the total available strength about 22%, independent of Q_a . These observations are of course particular for this given example and cannot be generalized.

The sensitivity of the cyclic interaction diagrams to the two choices of the degradation formulation for the sands (Eq. (6) and (7)) was studied. Figure 7 shows the diagrams for a pile length of 115m and a diameter of =48 inches. For this case it is noted that even with the significant differences in the degradation represented by both Eqs. the results are approximately equal. The highest differences corresponds to the case N=15, due to the very different initial values of degradation in the sands, but even in this case the results are within $\pm 6\%$.

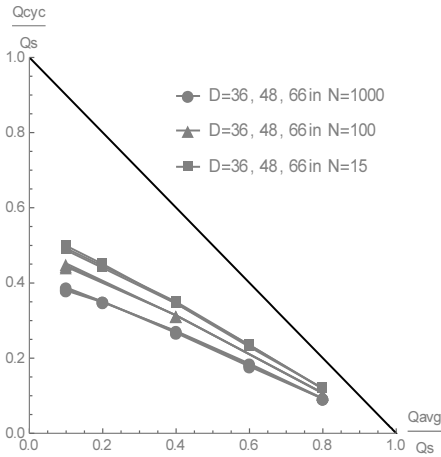


Figure 6. Cyclic interaction diagram for basic clay and first sand model.

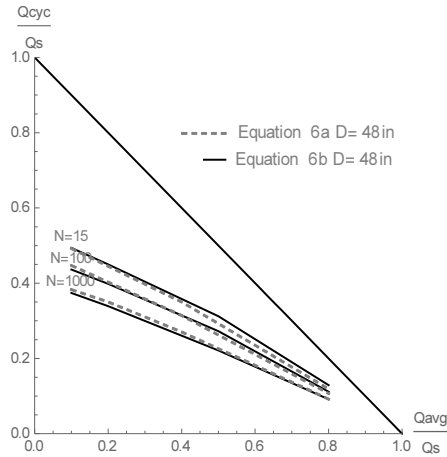


Figure 7. Cyclic interaction diagram for basic clay and second sand model.

In case that the load combinations acting on the given pile are not located inside the cyclic interaction diagram the diameter, length or number of the piles must be increased until the load combinations lay inside the corresponding diagram. The magnitude of the loads must be representative of the number of cycles used. It would be incorrect to use the maximum values of the oceanographic and/or seismic loads with for instance $N=1,000$ or $N=15$ respectively. It is recommended that for the ELE level of seismic loads (as defined in API RP 2EQ), the maximum value of the cyclic seismic action may be multiplied by for instance 0.65, (as it is done for the cyclic stress ratio estimation in the liquefaction evaluation) and use with $N=15$. For the oceanographic case, a representative value of the cyclic load in the 100-1000 cycles range could be defined or alternatively, the accumulation methods described in 4.3 can be used at the pile level with the post cyclic degraded axial capacity as the control parameter.

At the end of the analysis procedure a set of degraded or “post-cyclic” $t-z$ curves are obtained. From them a degradation factor (η_{min}) can be defined as $\eta_{min}=(t_{max \text{ post-cyclic}})/(t_{max \text{ static}})$ for each $t-z$ element. These reduction values correspond to the application of the specified number of cycles (N) with the highest value of the cyclic component ($Q_c \text{ max}$) obtained from the interaction diagram for a given level of average load (Q_a). If the cyclic component applied (Q_c) is lower than the maximum given in the interaction diagram, an increased η (less degradation) value could be linearly interpolated.

6. Conclusions

The computation of cyclic interaction diagrams for axial loads based on the effective stress ICP pile procedure was presented. The proposed method accounts for the progressive and cumulative degradation that develops along the pile shaft during a given number of cycles of constant amplitude cyclic axial load superimposed on an average load. The method can be easily modified to other load histories.

For the particular examples presented in an alternated clay-sand profile from the Mexican sector of gulf of Mexico, the normalized cyclic interaction diagrams showed small sensitivity to the pile diameter, number (m) of blocks in which the total number of

cycles is subdivided and details of the sand degradation model. In spite of this a key aspect is the proper characterization of the degradation of each soil strata under a set of cyclic DSS tests. Ideally those tests should be done under constant volume for clays and constant normal stiffness for sands. Alternatively a constant volume can be imposed on sands but the results may be too conservative. A representative level of preshearing should be applied, particularly for reconstituted sand samples. The cyclic interaction diagrams can be considered as an intermediate screening tool. If the cyclic effects are shown to be significant, their computation can be modified to better account for details of the applied load histories.

References

- [1] R. Bea, "Dynamic response of marine foundations," in *Proceedings of the Ocean Structural Dynamics Symposium '84*, Oregon, 1984.
- [2] K. A. Andersen, A. A. Puech and R. J. Jardine, "Cyclic resistant geotechnical design and parameter selection for offshore engineering and other applications," in *Proc. of TC 209 Workshop 18th ICSMGE*, Paris, 2013.
- [3] R. Jardine, F. Chow, R. Overy and J. Standing, *ICP Design Methods for Driven Piles in Sands and Clays*, London: Thomas Telford, 2005.
- [4] O. Benzaria, A. Puech and A. Le Kouby, "Effects of installation method on the static behaviour of piles in highly overconsolidated Flanders clay," in *Proc. of TC 209 Workshop 18th ICSMGE*, Paris, 2013.
- [5] API, *Recommended Practice for Geotechnical and Foundation Design Considerations - API RP 2GEO*, 2nd ed., American Petroleum Institute, 2014.
- [6] M. F. Randolph and S. M. Gourvenec, *Offshore Geotechnical Engineering*, 1st ed., Spon Press, 2011.
- [7] WS Atkins, "Cyclic degradation of offshore piles," OTO Report 2000/013, 2000.
- [8] U. Hoppe, "Computational Plasticity," in *Lecture Notes*, Ruhr Universitat Bochum, 2010.
- [9] L. L. Yaw, *Non Linear Static 1D Plasticity - Various forms of Isotropic hardening*, Walla Walla University, 2012.
- [10] M. Manzocchi, "Personal communication to R. Jardine in Appendix E," in "*Pile load testing performed for HSE cyclic loading study at Dunkirk, France - Volume 1.*" OTO 2000/0081., 1998.
- [11] K. H. Andersen, R. Dyvik, Y. Kikuchi and E. Skomedal, "Clay behaviour under irregular cyclic loading," in *Proc. of the 6th International Conference on the Behaviour of Offshore Structures*, London, 1992.
- [12] Norwegian Geotechnical Institute for Geohidra Consultores, "Cyclic DSS for a location in Gulf of Mexico", Internal report, 2017.
- [13] Instituto Mexicano del Petroleo for Geohidra Consultores "Criteria for seismic design for a location in Gulf of Mexico.", internal report. Ciudad de Mexico, 2017.